Published in final edited form as:
Mol Cell. 2012 March 9; 45(5): 680–695. doi:10.1016/j.molcel.2012.01.013.

Tex14, a Plk1 regulated protein, is required for kinetochore-microtubule attachment and regulation of the spindle assembly checkpoint

Gourish Mondal[1], **Akihiro Ohashi**[1], **Lin Yang**[1], **Matthew Rowley**[1], and **Fergus J Couch**[1,*]
[1]Department of Laboratory Medicine and Pathology, Mayo Clinic, Rochester, MN 55905, USA

SUMMARY

Proper assembly of kinetochores (KTs) during mitosis is required for bipolar attachment of spindle microtubules (MTs) and the accumulation of spindle assembly checkpoint (SAC) components. Here we show that testis expressed protein 14 (Tex14), which has been implicated in midbody function, is recruited to KTs by Plk1 in a Cdk1-dependent manner during early mitosis. Exclusion of Tex14 from kinetochores results in an inability to efficiently localize outer KT components, impaired KT-MT attachment, chromosome congression defects and whole chromosome instability. In addition, we demonstrate that phosphorylation of Tex14 by Plk1 during metaphase promotes APC^{Cdc20}-mediated Tex14 degradation. Inhibition of this phosphorylation event causes retention of Tex14 at KTs and results in delayed metaphase to anaphase transition and chromosome segregation defects. Our findings identify Tex14 as an important mediator of KT structure and function and the fidelity of chromosome separation.

Keywords

Tex14; kinetochore; Plk1; spindle assembly checkpoint

INTRODUCTION

Chromosome segregation during mitosis involves a dynamic interaction between spindle microtubules (MTs) and kinetochores (KTs), macromolecular complexes that localize at the centromeres of mitotic chromosomes. This interaction is required for bipolar attachment and tension between paired KTs and MTs and subsequent alignment of sister chromatids to the metaphase plate. The attachment of spindle MTs to KTs is monitored by the mitotic spindle assembly checkpoint (SAC), a surveillance mechanism that prevents premature separation of sister chromatids until all KTs are attached (Musacchio and Salmon, 2007; Khodjakov and Pines, 2010). At KTs the active checkpoint is associated with a wait anaphase signal that prevents activation of the anaphase-promoting complex/cyclosome (APC/C) (Kulukian et

*Correspondence: Fergus J. Couch, Ph.D., Department of Laboratory Medicine and Pathology, Mayo Clinic Stabile 2-42, 200 First Street SW, Rochester, MN 55905. Tel: (507)284-3623., couch.fergus@mayo.edu.

SUPPLEMENTAL INFORMATION:
Supplemental data include supplemental experimental procedures, four supplemental tables, supplemental figure legends, supplemental references, seven supplemental figures, and seven supplemental movies.

al., 2009), degradation of target proteins, and progression from metaphase to anaphase. Disruption of KT assembly, attachment of spindle MTs, or SAC activity often leads to chromosome mis-segregation or premature mitotic exit and aneuploidy, a hallmark of many solid tumors (Musacchio and Salmon, 2007).

KTs in vertebrates appear as trilaminar plate structures that assemble in a stepwise fashion during KT maturation (DeLuca et al., 2005; Liu et al., 2006; Wan et al., 2009). Unlike constitutively localized inner KT proteins, many outer KT proteins are recruited to KTs at the beginning of prophase and are maintained only through the satisfaction of the SAC or until mitotic exit. The outer KT contains many proteins involved in MT attachment including the KMN network containing the KNL1 complex, the MIS12 complex, and the NDC80 complex that forms MT attachment sites at KTs and is essential for end-on attachment (Cheeseman et al., 2006; Wan et al., 2009). The NDC80 complex components, Ndc80 (Hec1) and Nuf2, interact with MTs and are anchored to the KT through the Spc24 and Spc25 subunits (Cheeseman et al., 2006). These proteins interact with the NSL1 subunit of the MIS12 complex (Petrovic et al., 2010), and may be anchored to the inner KT by CENP-C (Cheeseman et al., 2004; Hemmerich et al., 2008). In contrast, the KNL complex is required for recruitment of SAC components (Musacchio and Salmon, 2007). These complexes and other regulatory components of the outer KT mediate MT attachment and tension and subsequent resolution of the SAC.

The Plk1 mitotic kinase, which interacts with Cdk1-phosphorylated consensus sequences on many docking proteins through a non-catalytic C-terminal “polo-box” (Qi et al., 2006; Wong and Fang, 2007), also influences the recruitment of proteins to outer KTs (Baumann et al., 2007; Kang et al., 2006). In addition, Plk1 has been implicated in regulation of the function of several outer KT proteins. For instance, Plk1-dependent phosphorylation of BubR1 has been associated with formation of the 3F3/2 epitope, a marker of intra-KT tension (Ahonen et al., 2005; Wong and Fang, 2005; Maresca and Salmon, 2009). However, while Plk1 has been implicated in regulation of outer KT maturation, the specific mechanisms behind these events remain largely undefined.

Studies of germ cells from Tex14 knockout mice have shown that Tex14 is required for spermatogenesis and male fertility and is involved in formation of intracellular bridges during cytokinesis (Greenbaum et al., 2006). Tex14 also competes with Alix and Tsg101 for binding to CEP55 at the midbody and inhibits the resolution of intercellular bridges during abscission in germ cells (Iwamori et al., 2010). Here we explored the influence of Tex14 on mitosis in somatic cells and found that Tex14 is also a novel component of mitotic KTs. We report that Tex14 is recruited to KTs by Plk1 where it regulates maturation of the outer KT and KT-MT attachment. In addition, we show that phosphorylation of Tex14 by Plk1 during metaphase is required for proteosome dependent degradation of Tex14 and transition from metaphase to anaphase. Based on our findings, we identify Tex14 as a dual target of Plk1 that mediates accurate chromosome segregation and whole chromosome stability.

RESULTS

Tex14 localizes to the KT during mitosis

Tex14 was recently identified as a component of the intercellular bridge and the midbody that is required for maintenance of normal cytokinesis (Greenbaum et al., 2006). To further examine the involvement of Tex14 in the mitotic process we studied the localization of endogenous Tex14 during mitosis by immunofluorescence staining of HeLa cells for Tex14 (Figure 1A) using an anti-Tex14 polyclonal antibody that was validated by western blot and immunofluorescence of Tex14 depleted cells. Tex14 levels were low in interphase cells but rapidly increased upon entry into mitosis. Tex14 was predominantly localized on KTs

throughout prophase, prometaphase and early metaphase (Figure 1A). However, Tex14 was substantially reduced at KTs during late metaphase and anaphase (Figure 1A) and partially relocalized to the midbody in telophase (Figure 1A), as previously reported (Greenbaum et al., 2006). These observations were confirmed by live cell imaging of 293T cells co-expressing EGFP-tagged Tex14 and H2B-mRFP (Supplemental movies- 1 and 2).

Tex14 interacts with Plk1 through polo box binding domains

The localization of Tex14 to mitotic structures prompted efforts to identify Tex14 binding proteins during mitosis. FLAG-tagged wild type-Tex14 (WT-Tex14) was immunoprecipitated from 293T cells following nocodazole treatment and Tex14 associated immune complexes were separated by SDS-PAGE (Figure 1B). Mass spectrometric analysis of immune complexes identified Plk1 as a Tex14 interacting protein. To confirm this interaction we conducted immunoprecipitation and western blot studies of endogenous Tex14 and Plk1 in 293T and HeLa cells aligned in prometaphase by nocodazole. A Tex14-Plk1 complex was consistently identified suggesting an interaction between these proteins during early mitosis (Figure 1C). Further studies using Plk1 fragments established that the C-terminal polo-box domain of Plk1 was necessary for the interaction with Tex14 (Figure S1A).

To map the location of Plk1 binding domains within Tex14, interactions between Plk1 and a series of GST-fusion proteins containing fragments of Tex14 (F1 to F4) and FLAG-tagged in-frame deletion mutants of Tex14 (G1–G10) were evaluated (Figure 1D). Tex14 fragments F2 and F3 interacted with Plk1 (Figure S1B), while Tex14 G5 and G6 in-frame deletion mutants, lacking a 294 amino acid region (581–875), failed to interact with Plk1 (Figure 1E). ClustalW analysis of Tex14 from various species identified six highly conserved consensus Plk1 polo-box binding domain (PBD) motifs (S-T/S-X) in this region of Tex14. All Ser and Thr residues in the Tex14 candidate PBD motifs were mutated to Ala in full-length Tex14 (PBD-1 to PBD-5) and the ability of the mutants to interact with Plk1 was evaluated. Tex14 PBD-1, containing mutations in two adjacent Tex14 PBD motifs (S608A-S609A-X and S611A-T612A-X) and Tex14 PBD-5 (S720A-T721A-T722A-X) displayed a reduced ability to interact with Plk1 (Figure 1F). In contrast, alteration of individual Ser or Thr residues (S-S/T-X) in the Tex14 PBD-1 [PBD-1-2 (S609A); PBD-1-4 (T612A)] and in the Tex14 PBD-5 [PBD-5-2 (T721A); PBD-5-3 (T722A)] had little effect on the Plk1 interaction (Figure S1C). These findings suggest a complex interaction between Plk1 and Tex14 involving the PBD-1 and PBD-5 regions of Tex14.

Cdk1 phosphorylation of Tex14 is required for the Tex14-Plk1 interaction

Since Plk1 binding to substrates is often dependent on initial phosphorylation by the Cdk1 priming kinase (Kang et al., 2006; Qi et al., 2006), the involvement of Cdk1 phosphorylation in the binding of Plk1 to Tex14 PBDs was evaluated. Western blotting of immunoprecipitates from monastrol treated 293T cells expressing FLAG-tagged Tex14 established that Tex14 interacted with Cdk1 during early phases of mitosis (Figure 2A). Additional studies using Tex14 G1 to G10 deletion mutants showed that only the G5 mutant failed to interact with Cdk1 (Figure 2B). Interestingly, PBD-1 and PBD-5 mutants and a PBD-1 and PBD-5 double mutant (PBD-(1+5)) did not disrupt Cdk1 binding to Tex14 (Figure S1C-E), suggesting that the Cdk1 binding site/s differs from the Plk1 binding sites. This is consistent with previous studies showing that Cdk1 phosphorylates and primes target PBDs for Plk1 binding but often binds directly to other domains of these proteins (Fabbro et al., 2005).

Next we evaluated the ability of Cdk1 to phosphorylate the Tex14 PBD-1 and PBD-5 Plk1 interaction sites. Cells aligned in prometaphase with nocodazole displayed Thr-

phosphorylation of Tex14 which was decreased following treatment with the Cdk1 inhibitor RO-3306 (Figure 2C). Similarly, compared to wildtype Cdk1, a D146A dominant negative Cdk1 (Cdk1-DN) mutant was associated with a substantial reduction in Tex14 Thr phosphorylation (Figure S1D,F). There was no difference in Ser-phosphorylation under these conditions (data not shown). In addition, the PBD-1 and PBD-5 Tex14 mutants showed reduced Cdk1-dependent phosphorylation (Figure 2C and S1D-F). Thus, Thr-phosphorylation of Tex14 in prometaphase appears to be predominantly associated with Cdk1 associated phosphorylation of Plk1 binding sites. Furthermore, since the PBD-1, PBD-5 and PBD-(1+5) Tex14 mutants and Cdk1-DN reduced both Cdk1-dependent phosphorylation of Tex14 and Plk1 interaction with Tex14 in prometaphase (Figure 2C and S1D-F), phosphorylation of Tex14 PBD-1 and PBD-5 by the Cdk1 priming kinase appears to be required for the Tex14-Plk1 interaction.

Localization of Tex14 to KTs is dependent on Plk1 binding

Since Tex14 localized to KTs during early mitosis (Figure 1A), we assessed the influence of Plk1 on the KT localization of Tex14. Using immunofluorescence staining we showed that only the G5 and G6-Tex14 in-frame deletion mutants, that are deficient in Plk1 binding, failed to localize efficiently to KTs during prometaphase (Figure 2D and Figure S2A). Similarly the PBD-1 and PBD-5 mutants, which also disrupt Plk1 binding, interfered with Tex14 localization to KTs (Figure 2D), whereas the PBD-2, PBD-3, and PBD-4 mutants, that had no effect on Plk1 binding, did not influence KT localization of Tex14 (Figure S2B). Tex14 also failed to localize to KTs following siRNA depletion of Plk1 (Figure 2D). These results suggest that Tex14 localizes to KTs through an interaction with Plk1. Interestingly, we also found that Tex14 shRNA had no effect on Plk1 localization to KTs (Figure 2D) as shown by quantitation of Tex14 and Plk1 levels at KTs (Figure S2C), suggesting that Tex14 has no influence on localization of Plk1.

Next, we used immunoprecipitation of Tex14 from cells aligned in prometaphase by monastrol to show that Tex14 forms complexes with several KT associated proteins including Mad2, Cdc20, CENP E, BubR1, Hec1 and the Plk1 and Cdk1 signaling kinases (Figure 2E and S2D). Reciprocal immunoprecipitation of endogenous Tex14 with kinetochore markers such as Mad2 and CENP E was also observed (Figure S2E). Based on these findings we evaluated the influence of Plk1 on the interaction of Tex14 with KT markers. The Plk1 binding deficient Tex14 mutant PBD-(1+5) exhibited substantially reduced interactions with Plk1, CENP E, BubR1, and Hec1 (Figure 2E and S2D), consistent with an inability of Tex14 to localize to KTs. However, the PBD-(1+5) mutant maintained the ability to form complexes with Cdc20 and Mad2 in mitotic cells (Figure 2E), suggesting that Tex14 may also interact with both Mad2 and Cdc20 through another mechanism.

Tex14 is required for recruitment of outer KT proteins

Because Tex14 localizes to KTs and interacts with KT components, we assessed the impact of Tex14 exclusion from KTs on the composition of the outer KT plate. Following depletion of Tex14 from HeLa and 293T cells using three individual Tex14 shRNAs (Figure S3A), the localization of a series of KT components to KTs during early mitosis was evaluated by immunofluorescence. Depletion of Tex14 resulted in significant displacement of the Ndc80 complex members Hec1, Nuf2, Spc24 and Spc25, which are involved in KT-MT attachment (Figure 3A and Figure S3B-E). Since recruitment of the Ndc80 complex to kinetochores is significantly influenced by reduced levels of the Mis12 complex (Cheeseman et al., 2004), we explored the impact of Tex14 depletion on localization of Mis12 complex components. In the absence of Tex14, NSL1 was substantially reduced at KTs, whereas the Mis12 protein appeared to be unaffected (Figure 3A,B). Similarly, the CENP C, CENP A, and CENP I centromeric and inner KT proteins were not reduced or mislocalized (Figure 3A and Figure

S3F,G). Consistent with these findings, shRNA resistant Tex14 (SR-Tex14) (Figure S3H) rescued the localization of KT markers influenced by Tex14 depletion (Figure S3C-E, I). Quantitation of the average KT intensity of several of these markers confirmed these observations (Figure 3C). Together these observations suggest that the inefficient recruitment of proteins to outer KTs during mitosis in the absence of Tex14 may be associated with the incomplete assembly of the MIS12 complex.

Given, the impact on outer KT markers, we also evaluated the influence of Tex14 depletion on KT-associated SAC components. Mad2 and Mps1 were strikingly reduced at KTs (Figure 3A–C and S3J). In addition, Mad1 was displaced from a subset of KTs (Figure 3A–C) and both Mad1 and CENP E were reduced in intensity at KTs (Figure 3A–C). In contrast, Tex14 depletion had no effect on localization of Cdc20, Bub1, BubR1, ZW10 and the Aurora B and Plk1 signaling kinases (Figure 3A). To rule out the possibility that mislocalization of KT markers, resulted from protein turnover during the prolonged prometaphase delay in Tex14 depleted cells, we evaluated localization of KT markers in response to treatment with nocodazole and the MG132 proteasome inhibitor (6hr). MG132 treatment did not alter the mislocalization of KT markers such as Mad2 (Figure S3K), again suggesting an active role for Tex14 in recruitment of outer KT markers.

To determine whether these effects were dependent on localization of Tex14 at the KT, we evaluated the influence of mutations that disrupt Plk1-dependent recruitment of Tex14 to the KT on the localization of the KT markers. The PBD-(1+5) Tex14 mutant that failed to localize to KTs, influenced localization of MIS12 and NDC80 complex proteins (Figure 3A and S3B,C,J,L,M), but not inner-KT proteins such as CENP I and CENP C (Figure S3F,G), similarly to Tex14 depletion. In addition, the G5, PBD-1 and PBD-5 Tex14 mutants significantly displaced Mad2 from KTs (Figure S4A), and reduced the levels of Mad1 (Figure S4B) and CENP E (Figure S4C), while a G3 control mutant had no influence on these markers (Figure S4A–C). In contrast, these mutations had no influence on Cdc20, Bub1, BubR1, and Aurora B localization (Figure S4D and S5A–D), suggesting that Plk1-dependent recruitment of Tex14 to KTs regulates the KT localization of a specific subset of outer KT proteins. Since Mad2 antibodies may fail to detect C-Mad2 at KTs we also assessed localization of Myc-tagged Mad2 (Figure S5E) in Tex14 or Plk1 depleted cells or PBD-(1+5) expressing cells. Consistent with previous results we observed substantial displacement of Mad2 from KTs when immunostaining with an anti-Myc antibody (Figure S5F,G). Live cell imaging of 293T cells co-expressing EGFP-tagged Mad2 and mCherry α-tubulin also showed reduced levels of Mad2 at KTs in the absence of Tex14 (supplemental movies- 3 and 4). In addition, quantitation of Mad2 at KTs showed that Mad2 levels at KTs were substantially reduced by Tex14 depletion, consistent with the effects of reversine, Plk1 siRNA (Ahonen et al., 2005) and Mad2 siRNA (Figure S6A,B). However, Tex14 depletion, but not MPS1 inhibition or Mad2 siRNA, reduced Mad1 levels at KTs (Hewitt et al., 2010) (Figure S6A), consistent with a broad influence of Tex14 on the structure of the outer KT. We also used a biochemical approach to show that depletion of Tex14 or expression of the Tex14 PBD-(1+5) and G5 mutants reduced the ability of Mad1 to form complexes with ectopically expressed Myc-Mad2 in nocodazole treated cells, consistent with the effects of the Mps1 inhibitor reversine and Plk1 siRNA (Figure 3D). Likewise depletion of Tex14 from nocodazole aligned cells substantially reduced the interaction between endogenous Mad1 and Mad2 (Fig S5H). We conclude that Tex14 localization to KTs is important for recruitment of a number of proteins including Mad1 and Mad2 to the outer kinetochore.

Next, we evaluated the recruitment of KT markers in response to disruption of Plk1 by siRNA depletion or expression of kinase dead K82M Plk1 (KD-Plk1) (Seong et al., 2002) to determine if the effects of Plk1 inactivation were consistent with those induced by exclusion of Tex14 from KTs. Plk1 siRNA reduced localization of Mad1, Mad2, and CENP-E at KTs

(Figure S4A-D), but had no influence on BubR1 and Bub1 localization (Figure S4D and S5B). KD-Plk1 also partially reduced the levels of Mad1, Mad2, CENP-E and Cdc20 (Figure S4A-D and S5A). Together these findings indicate that Plk1-dependent localization of Tex14 at KTs is required for proper localization of some but not all components of the outer KT plate.

Tex14 is required for formation of the Plk1-dependent 3F3/2 phosphoepitope at KTs

Since Plk1 regulates the recruitment of Tex14 to KTs we investigated whether Tex14 mediates the influence of Plk1 on KTs. Phosphorylation of BubR1 by Plk1 and other mitotic kinases creates a series of phosphoepitopes at the KT that mediate spindle attachment, spindle tension, and checkpoint activity (Ahonen et al., 2005; Qi et al., 2006; Wong and Fang, 2005; Wong and Fang, 2007). In particular, Plk1-mediated phosphorylation of BubR1 at unattached KTs has been associated with the formation of the 3F3/2 phosphoepitope, a marker that is removed from KTs following KT-MT attachment and establishment of intra-KT tension (Ahonen et al., 2005; Huang and Yen, 2009; Wong and Fang, 2007; Maresca and Salmon, 2009). Here we used immunofluorescence to show that depletion of Tex14 or expression of PBD-(1+5) significantly inhibited 3F3/2 formation in prometaphase cells (Figure 3E), while shRNA-resistant Tex14 (SR-Tex14) reconstituted the 3F3/2 phospho-epitope (Figure 3E). Reduced levels of the BubR1-associated 3F3/2 phospho-epitope were also observed in BubR1 immunoprecipitates from monastrol treated cells expressing PBD-(1+5) or Tex14 shRNAs (Figure 3F). Consistent with these findings, inhibition of Cdk1 and Plk1 kinase activity has previously been shown to have similar effects on 3F3/2 (Wong and Fang, 2005; Wong and Fang, 2007). Importantly, the influence of Tex14 on 3F3/2 was not associated with reduced levels of Plk1 or BubR1 at KTs because Tex14 depletion had no effect on Plk1 localization (Figure S2C) or BubR1 localization (Figure 3A and S4D) to KTs. However, immunoprecipitation and western blotting revealed that Tex14 depletion had no influence on the interaction of Plk1 with Bub1 but substantially diminished the interaction between Plk1 and BubR1 in prometaphase cells (Fig S6C). This specific effect on the Plk1-BubR1 interaction suggests that Tex14 may influence the ability of Plk1 to interact with certain substrates at KTs.

Absence of Tex14 from the KT causes chromosome congression defects

Since Tex14 is required for efficient localization of several proteins to the outer KT, we evaluated whether Tex14 is required for KT function.Immunofluorescence studies detected an increased frequency of chromosome congression defects, consisting of multiple unattached and unaligned chromosomes, in mitotic cells depleted for Tex14 or expressing the Tex14 PBD-1 mutant (Figure 4A) relative to controls. To better understand these mitotic defects 293T cells expressing RFP-tagged H2B were followed by live-cell time-lapse microscopy after depletion of Tex14 by shRNA. Tex14 depleted cells again displayed chromosome congression defects and significant delays in prometaphase. Quantitation of live-cell imaging studies revealed that 60% of these cells exhibited delays of at least 1hr during prometaphase leading to prolonged delay over a 6hr period (10%), premature exit from mitosis associated with DNA decondensation (12%), or apoptosis (38%) (Figure 4B). Separately, quantitation of chromosome numbers in colcemid treated metaphase spreads of Tex14 depleted cells detected elevated levels of aneuploidy (18%), likely resulting from defects in chromosome segregation (Figure 4C and S6D). Thus, absence of Tex14 from KTs is associated with significant mitotic defects originating in early mitosis.

Depletion of Tex14 has also been implicated in failure of cytokinesis in mouse spermatocytes (Greenbaum et al., 2006). To confirm this effect in somatic cells we depleted Tex14 from HeLa cells, and followed cells that had escaped the initial prometaphase delay due to absence of Tex14, through telophase and cytokinesis by live-cell imaging. The

majority of these cells (68%) suffered a delay or failure of cytokinesis (Figure S6E,F), consistent with the increased polyploidy observed in Tex14 depleted cells relative to controls (Figure 4C). Thus, loss or inactivation of Tex14 may lead to aneuploidy due to chromosome segregation issues following chromosome congression defects and/or polyploidy due to inefficient cytokinesis.

Tex14 influences KT-MT attachment and tension

The delays in chromosome congression, the unaligned chromosomes, and the reduced levels of NSL1 and the components of the Ndc80 complex in cells with reduced levels of Tex14 at KTs, suggested a role for Tex14 in establishing KT-MT attachment and/or KT tension. To explore the influence of Tex14 on KT-MT attachment we directly assessed the integrity of bipolar end-on MT attachments to KTs in Tex14 deficient cells. Immunofluorescence analysis of Tex14 depleted cells detected unattached KTs, including those located near spindle poles that failed to align at the developing metaphase plate (Figure 4D). In addition, a significant difference in end-on inter-KT distance was observed in the absence of Tex14 (Figure 4E,F), consistent with a failure to induce tension following aberrant MT attachment. Furthermore, we evaluated the influence of Tex14 on Aurora B mediated CENP-A Ser-7 phosphorylation, which has been implicated as a marker of intra-KT tension following bipolar attachment of KTs to MTs (Liu et al., 2009). Initially, we confirmed that unmodified cells displayed high levels of phospho-CENP-A at KTs during early prometaphase (Figure 4G), but substantially diminished phospho-CENP-A levels during late prometaphase and metaphase (Figure 4G). In contrast, late prometaphase cells expressing PBD-(1+5) retained high levels of phospho-CENP-A at KTs (Figure 4G) suggesting that reduced levels of Tex14 prevents tension-associated separation of Aurora B from CENP-A at centromeres. We further established that Tex14 is required for normal KT-MT attachment and chromosome congression by performing live-cell imaging of 293T cells co-expressing YFP-CENPA and mCherry α-tubulin and treated with Tex14 shRNA and controls (supplemental movies-5 and 6). A large proportion (10 of 14) of Tex14 depleted cells exhibited attachment defects with severe chromosome congression problems and prometaphase delay. Furthermore, extension of prometaphase for 2–3hrs with MG132 treatment did not rescue these defects in Tex14 depleted cells as only 2 of 15 cells completed error-free chromosome congression and alignment (supplemental movie-7). Together these observations suggest that depletion of Tex14 results in a disorganized outer KT and impairment of KT signaling necessary for MT to KT attachment, intra-KT tension, and error-free chromosome alignment and segregation.

Tex14 influences the SAC

Failure of KT-MT attachment and intra-KT tension is usually associated with continued SAC signaling in prometaphase and production of a “wait anaphase” signal that inhibits APC/C function. Thus, we expected to observe an active checkpoint in the absence of Tex14. However, since exclusion of Tex14 from KTs also reduced levels of Mad2, an important mediator of SAC signaling (Musacchio and Hardwick, 2002; Shah et al., 2004), we reasoned that Tex14 depletion might disrupt SAC activity. Treatment of Tex14 depleted cells with nocodazole to induce SAC activity enriched cells in prometaphase, consistent with checkpoint activation (Figure 5A). However, lower proportions of mitotic cells were observed relative to controls (Figure 5A) suggesting a weakened mitotic checkpoint due to reduced levels of SAC components such as Mad2. Depletion of the SAC mediators, Mad2 and BubR1 (Figure 5B), alone and in combination with Tex14 depletion, had similar effects on SAC activity as Tex14 depletion (Figure 5A). The small differences in these effects were likely due to differences in the efficiency of the various small interfering RNAs. These findings suggest that reduced levels of Tex14 at KTs reduce SAC activity by partial mislocalization of Mad2, and perhaps other SAC mediators.

Phosphorylation of Tex14 Ser431 by Plk1 promotes Tex14 depletion

While further evaluating the interaction between Tex14 and Plk1 we observed that expression of wildtype Plk1 but not KD-Plk1 was associated with a substantial reduction in Tex14 protein levels in nocodazole treated cells (Figure 6A, first panel and S7A). This effect was consistent with a rapid reduction in Tex14 levels at KTs during late prometaphase and metaphase (Figure 1A). In addition, the reduced Tex14 levels were coincident with increased serine-phosphorylation of Tex14 by wildtype Plk1, but not KD-Plk1, in cells synchronized in prometaphase by nocodazole (Figure 6B). To further explore this relationship we mapped sites of Plk1-dependent phosphorylation during prometaphase and metaphase to the overlapping region of the F2 and G3 fragments of Tex14 (amino acids 407–439). Alanine mutagenesis of conserved serine residues showed that a Ser431Ala (S431A) mutant significantly reduced serine phosphorylation of Tex14 during prometaphase (Figure 6B). Furthermore, S431A significantly increased Tex14 levels in the presence of WT-Plk1, whereas an S456A mutant from outside the region had no influence (Figure 6A). Immunofluorescence studies detected high levels of the S431A-Tex14 mutant at KTs and spindle poles during prometaphase and metaphase and at the central spindle during telophase, coincident with Plk1, whereas wildtype Tex14 was reduced or absent from all structures after prometaphase (Figure S7B-E). Importantly, wildtype Tex14 in the presence of KD-Plk1 displayed similar staining as S431A-Tex14 (Figure S7B–E), suggesting that phosphorylation of Tex14 at Ser431 by Plk1 during late prometaphase/metaphase promotes rapid reduction in the overall and KT-specific levels of Tex14.

To verify these findings we generated a phospho-specific antibody against Phospho-Ser431 of Tex14. Immunoblotting with this antibody detected WT-Tex14 at low levels in unsynchronized cells, moderate levels in cells aligned in prometaphase by nocodazole treatment and high levels in cells aligned in late prometaphase/early metaphase by MG132 treatment or after 30 min release from Nocodazole block (Figure 6C,D). However, no phosphorylation of the S431A-Tex14 mutant protein was observed under any conditions with this antibody (Figure 6C,D). Immunofluorescence studies with the pSer431 antibody also detected WT-Tex14 at KTs during metaphase (Figure 6E), but not during early prometaphase prior to Plk1-dependent Ser phosphorylation of Tex14 or during anaphase when Tex14 is largely absent (Figure 6E). Likewise, the antibody did not detect S431A-Tex14 at other stages of mitosis (Figure S7F). Importantly, while high levels of Plk1-dependent Ser431 phosphorylation were associated with reduced levels of Tex14 protein in late prometaphase (Figure 6C, lanes 2 and 3), limited Ser431 phosphorylation resulting from expression of KD-Plk1 or the S431A Tex14 mutant or treatment with the Plk1 inhibitor BI-2536 was associated with stabilization of Tex14 (Figure 6D). To verify this finding, we compared Ser431 phosphorylation and Tex14 levels at several timepoints between prometaphase (nocodazole arrest) and anaphase in 293T cells. Phosphorylation of Tex14 on Ser431 occurred during late prometaphase and was strongly associated with a rapid diminution in Tex14 levels over a 40 min period as cells progressed through prometaphase (~0–20min) and entered metaphase (~20–40 min) and early anaphase (~50 min onward) (Figure 6F).

In support of these observations we found that Ser431Asp (S431D) and Ser431Glu (S431E) phospho-mimic mutants of Tex14 were barely detectable at KTs during prometaphase, in contrast to WT-Tex14, unless cells were treated for 2–3 hrs with the MG132 proteasome inhibitor (Figure 6G). Similarly, we showed that mutation of a Tex14 conserved D-box motif (aa 527-RxxLxxxxN-535) stabilized Tex14 during metaphase (Figure 6C). As this suggested the involvement of APC/C mediated proteosome degradation in Tex14 turnover, we evaluated interactions between Tex14 and Cdc27, an APC/C component, and between Tex14 and Cdc20, an APC/C activator. Both S431A and the D-box mutant substantially decreased the interaction between Cdc27 and Tex14 suggesting that a D-box mediated

interaction of the APC/C complex with Tex14 is in part responsible for S431-phosphorylation dependent Tex14 removal from KTs. In contrast, no effect of these mutants on the interaction with Cdc20 was observed possibly because other domains of Tex14 mediate this interaction (Figure 6C). Taken together these results indicate that Plk1 phosphorylation of Ser431 on Tex14 during late prometaphase and metaphase promotes the rapid depletion of Tex14 from KTs.

APC/C^{Cdc20} degradation of Tex14 is required for metaphase to anaphase transition

We further evaluated the influence of APC/C^{Cdc20} and APC/C^{Cdh1} complexes on Tex14 levels. Protein lysates were collected from Cdc20, Cdh1 or control shRNA treated 293T cells at several timepoints after entry into early prometaphase (7 hrs after release from a double thymidine block; Set 1) and after release from a prometaphase arrest (12 hrs of nocodazole treatment; Set 2) (Figure 7A,B). Consistent with our previous findings, Tex14 levels in untreated cells were elevated in prometaphase and then rapidly reduced in metaphase and anaphase after release from Nocodazole, similarly to phospho-H3 and Cyclin B1 (Figure 7A). Next, we used equal numbers of Cdc20 and Cdh1 depleted mitotic cells and control cells (normalized using phospho-H3) for immunoblotting to show that depletion of Cdc20 was associated with stabilization of Tex14 (Figure 7A), whereas depletion of Cdh1 did not influence Tex14 levels (Figure 7A). Similarly, immunofluorescence analysis revealed that late prometaphase and metaphase cells depleted for Cdc20 retained Tex14 and Mad2 at a subset of KTs (Figure 7C,D and S7G). This is consistent with the recent finding that cells from a *cdc20* hypomorphic mouse model display increased chromosome misalignment events at the metaphase plate (Malureanu et al., 2010). Thus, the rapid degradation of Tex14 during metaphase appears to be in-part mediated by APC/C^{Cdc20}.

Since the S431A mutant influenced the levels of Tex14 during metaphase, we evaluated the influence of the mutant on the localization of Tex14 to mitotic structures. S431A-Tex14 and WT-Tex14 in the presence of KD-Plk1, but not WT-Tex14 in the presence of WT-Plk1, localized to KTs and spindle poles during metaphase, to the central spindle during anaphase, and to the midbody during telophase and cytokinesis (Figure S7C–E). The detection of Tex14 at these structures suggests that Tex14 may be involved in centrosome, KT and midbody function, but it is also possible that the protein is inappropriately redistributed when stabilized. Next we assessed the impact of Tex14 stabilization on mitotic progression by live-cell time-lapse microscopy of 293T cells expressing RFP-tagged H2B along with S431A-Tex14 or WT-Tex14 or a vector control. Delays in the transition from prometaphase to metaphase and from metaphase to anaphase were observed in the presence of S431A-Tex14 (Figure 7E). Similarly, overexpressed WT-Tex14, which was not efficiently removed from KTs during metaphase by endogenous Plk1 (Figure 6D, lane 4), caused a substantial delay in mitotic transition (Figure 7E). Furthermore, 30% of S431A-Tex14 expressing cells and only 4.5% of control cells displayed either premature mitotic exit (DNA decondensation) or cell death during mitosis, possibly due to accumulated mitotic defects (Figure 7F and S7H). Thus, Plk1-dependent S431 phosphorylation, which is associated with depletion of Tex14 and removal of Tex14 from KTs, appears to serve as an important regulator of the prometaphase to metaphase and metaphase to anaphase transitions.

DISCUSSION

Plk1 recruits Tex14 to KTs

While Tex14 has been implicated in regulation of abscission during cytokinesis (Iwamori et al., 2010), here we introduce Tex14 as a novel Plk1 interacting partner and an important regulator of outer KT structure and function during mitosis. During early mitosis Plk1 interacts with consensus PBD-motifs in Tex14, in a Cdk1-dependent manner, and localizes

Tex14 to KTs. In this way, Tex14 resembles a number of other Plk1 binding partners, such as PICH and PBIP1, that interact with Plk1 through Cdk1 phosphorylated PBDs and are localized to KTs during early mitosis (Baumann et al., 2007; Neef et al., 2007; Qi et al., 2006). Here we show that the interaction between Plk1 and Tex14 is dependent on several Tex14 PBDs. While, mutation of individual PBDs in Tex14 partially reduces Cdk1-dependent phosphorylation levels and inhibits the ability of Tex14 to interact with Plk1 and to localize to KTs, mutation of all identified PBDs has a much more significant impact on binding. Whether the individual PBDs function independently and have specific temporal effects on Tex14 recruitment to KTs and/or on Tex14 function remains to be determined. Interestingly, recent studies have shown that many Plk1 binding partners do not contain PBDs (Santamaria et al., 2011). This raises the possibility that additional Plk1 binding sites, such as sites in the deleted region of the G6 in-frame deletion mutant that does not contain PBD1 or PBD5 or consensus Plk1 binding sites, but disrupts the Plk1 interaction, may also influence the Tex14 interaction with Plk1.

Co-dependent Tex14 and Plk1 function at KTs

Previous reports suggest that Plk1 and the Plk1 interactor, PICH, are co-dependent for KT and chromatid localization (Baumann et al., 2007). Likewise PBIP1, which also binds to Plk1 in a Cdk1-dependent manner, is required for the KT localization of Plk1 (Kang et al., 2006). Because of these observations, we evaluated whether Tex14 and Plk1 were co-dependent for KT localization. We found that localization of Tex14 to KTs is dependent on Plk1 binding but appears to be independent of Plk1 kinase activity, since a kinase-inactive form of Plk1 efficiently localized Tex14 to KTs (Figure S4A–D, S5A,B). In contrast, Plk1 localization to KTs is not dependent on the interaction with Tex14. However, our finding that Plk1 is unable to generate the 3F3/2 BubR1-associated phosphoepitope at KTs in the absence of Tex14, when both Plk1 and BubR1 are present at KTs, suggests that Tex14 influences Plk1 kinase activity at KTs. Whether the inability to generate the 3F3/2 phosphoepitope is caused by physical displacement of these proteins at KTs or a direct influence on Plk1 kinase activity remains to be determined. Should Tex14 function as a scaffold for Plk1 or a co-activator of Plk1 at KTs, it seems likely that phosphorylation of a broad array of Plk1 targets at KTs may be altered.

While Plk1 and Tex14 may have co-dependent functions at KTs during prometaphase, our data show that Plk1 also has a feedback regulatory effect on Tex14 at KTs during metaphase. Specifically, we show that Ser431 phosphorylation of Tex14 by Plk1 is required for rapid removal of Tex14 from KTs during metaphase. The retention of Tex14 at KTs during metaphase following inhibition of S431 phosphorylation disrupts the metaphase to anaphase transition. This type of feedback regulation of Plk1 substrates at KTs, as reported for PBIP1, has been identified as a switch that mediates the transition between phases of mitosis (Kang et al., 2006). Thus, Plk1 has a bimodal regulatory influence on Tex14 during mitosis.

Tex14 is required for assembly of outer KT components that regulate KT-MT attachment and SAC activity

Cells in which Tex14 is not localized to KTs fail to efficiently align chromosomes during mitosis. We found that inter-centromeric distances between paired KTs decreased and that unaligned centrophilic KTs exhibited Aurora B dependent Ser7 phosphorylation of CENP A when Tex14 was excluded from KTs, consistent with an absence of intra-centromeric tension due to defective KT-MT attachment (Liu et al., 2009). In addition, we determined that a subset of outer-KT proteins including components of the MIS12 and NDC80 complexes, such as Hec1, that is directly involved in KT-MT attachment (Ahonen et al., 2005; DeLuca et al., 2005; Wan et al., 2009), were considerably reduced at Tex14 deficient

KTs. The reduction in levels of these factors is consistent with the observed spindle attachment and tension defects and the chromosome congression errors observed in the absence of Tex14. Together these observations suggest that Tex14 is an important component of prometaphase KTs that is required for the structural assembly of the outer KT and subsequent MT attachment. Importantly, Tex14 depleted cells only displayed a partial reduction in the levels of certain outer-KT proteins, perhaps due to incomplete depletion of Tex14 by shRNAs or because Tex14 is not absolutely required for recruitment and retention of these outer-KT factors. As a result Tex14 depleted cells display milder and/or a lower frequency of chromosome congression defects than cells depleted for NDC80 or MIS12 complex components (Przewloka et al., 2007).

In keeping with the disruption of outer KTs, absence of Tex14 also affected a subset of SAC components. Interestingly, we observed a specific displacement of Mad2 from all Tex14 deficient KTs, in contrast to a partial mislocalization and/or reduction in levels of Mad1. Similar mislocalization of Mad2 from KTs has been observed in the absence of other Plk1 partners (Baumann et al., 2007; Kang et al., 2006) and following loss or inactivation of Mps1, which is recruited to KTs through the NDC80 complex (Hewitt et al., 2010; Santaguida et al., 2010). Since we observed reduced Mps1 protein levels at KTs in the absence of Tex14 it is possible that the effect on Mad2 is fully accounted for by Mps1 mislocalization. Further studies are needed to resolve the mechanism by which Tex14 influences Mad1 and Mad2 function during mitosis. Importantly, even though SAC components such as Mad1 and Mad2 were reduced at KTs, Tex14 depleted cells displayed some checkpoint activity in the presence of a Nocodazole challenge (Figure 5A). It is likely that the reduced levels of SAC mediators at KTs following depletion of Tex14 were sufficient to maintain a weak checkpoint in the absence of KT-MT attachment. However, the associated delays were insufficient for resolution of the KT-MT attachment defects caused by the extensive remodeling of outer KTs following depletion of Tex14. Overall, the combination of inefficient MT-KT attachment and partial disruption of SAC signaling caused by exclusion of Tex14 from KTs resulted in significant chromosome congression defects, delays during prometaphase and subsequent aneuploidy, polyploidy or cell death.

Tex14 is removed from KTs during late metaphase following phosphorylation by Plk1

As noted above, removal of Tex14 from KTs during late prometaphase and metaphase is mediated by Plk1 dependent Ser431 phosphorylation. This phosphorylation event is associated with D-box mediated and APC/C^{Cdc20}-dependent proteasomal degradation of Tex14. Since, Cdk1-dependent recruitment of Tex14 to KTs is no longer active at this stage of mitosis, the overall effect is a rapid reduction in Tex14 levels at KTs. This rapid reduction in Tex14 levels at this stage of mitosis has also been reported for several markers, including Mad2 and Bub3, that are involved in mediating SAC activity (DeLuca et al., 2003). Consistent with these findings disruption of Tex14-S431 phosphorylation results in retention of Tex14 at KTs during late prometaphase and metaphase. Likewise, overexpression of Tex14 leads to elevated levels of Tex14 at KTs, possibly by saturating the machinery that removes Tex14. The maintenance of Tex14 at KTs during metaphase results in stabilization of Cyclin B1 and securin (data not shown) and delayed transition from metaphase to anaphase. Furthermore, in contrast to Tex14 depletion, which causes defects in KT-MT attachment, and chromosome congression leading to cell death and chromosome segregation issues, retention of Tex14 at KTs predominantly results in premature mitotic exit, apoptosis or downstream cytokinesis defects.

Overall our data suggest a model whereby the levels of Tex14 at KTs during mitosis are tightly regulated by Plk1. While Plk1-dependent recruitment of Tex14 to KTs is required during early mitosis to promote KT-MT attachment, the removal of Tex14 following alignment of chromosomes and satisfaction of the SAC is equally important for completion

of karyokinesis (Figure 7G). Furthermore, since Tex14 is an important regulator of karyokinesis and is amplified and overexpresssed in breast tumors (Barlund et al., 2000; Sinclair et al., 2003), Tex14 may function like Mad2 and other mitotic regulators to regulate cancer development and progression.

EXPERIMENTAL PROCEDURES

See Supplemental Material

Supplementary Material

Refer to Web version on PubMed Central for supplementary material.

Acknowledgments

We thank James E. Tarara for assistance with live cell imaging and confocal microscopy and Jan van Deursen for the gift of antibodies. This work was supported by National Institutes of Health grant, CA87898. G. Mondal was supported by a grant from the Komen Foundation for the Cure.

References

Ahonen LJ, Kallio MJ, Daum JR, Bolton M, Manke IA, Yaffe MB, Stukenberg PT, Gorbsky GJ. Polo-like kinase 1 creates the tension-sensing 3F3/2 phosphoepitope and modulates the association of spindle-checkpoint proteins at kinetochores. Curr Biol. 2005; 15:1078–1089. [PubMed: 15964272]

Barlund M, Monni O, Kononen J, Cornelison R, Torhorst J, Sauter G, Kallioniemi OP, Kallioniemi A. Multiple genes at 17q23 undergo amplification and overexpression in breast cancer. Cancer Res. 2000; 60:5340–5344. [PubMed: 11034067]

Baumann C, Korner R, Hofmann K, Nigg EA. PICH, a centromere-associated SNF2 family ATPase, is regulated by Plk1 and required for the spindle checkpoint. Cell. 2007; 128:101–114. [PubMed: 17218258]

Cheeseman IM, Chappie JS, Wilson-Kubalek EM, Desai A. The conserved KMN network constitutes the core microtubule-binding site of the kinetochore. Cell. 2006; 127:983–997. [PubMed: 17129783]

Cheeseman IM, Niessen S, Anderson S, Hyndman F, Yates JR 3rd, Oegema K, Desai A. A conserved protein network controls assembly of the outer kinetochore and its ability to sustain tension. Genes Dev. 2004; 18:2255–2268. [PubMed: 15371340]

De Antoni A, Pearson CG, Cimini D, Canman JC, Sala V, Nezi L, Mapelli M, Sironi L, Faretta M, Salmon ED, et al. The Mad1/Mad2 complex as a template for Mad2 activation in the spindle assembly checkpoint. Curr Biol. 2005; 15:214–225. [PubMed: 15694304]

DeLuca JG, Dong Y, Hergert P, Strauss J, Hickey JM, Salmon ED, McEwen BF. Hec1 and nuf2 are core components of the kinetochore outer plate essential for organizing microtubule attachment sites. Mol Biol Cell. 2005; 16:519–531. [PubMed: 15548592]

DeLuca JG, Howell BJ, Canman JC, Hickey JM, Fang G, Salmon ED. Nuf2 and Hec1 are required for retention of the checkpoint proteins Mad1 and Mad2 to kinetochores. Curr Biol. 2003; 13:2103–2109. [PubMed: 14654001]

Fabbro M, Zhou BB, Takahashi M, Sarcevic B, Lal P, Graham ME, Gabrielli BG, Robinson PJ, Nigg EA, Ono Y, et al. Cdk1/Erk2- and Plk1-dependent phosphorylation of a centrosome protein, Cep55, is required for its recruitment to midbody and cytokinesis. Dev Cell. 2005; 9:477–488. [PubMed: 16198290]

Greenbaum MP, Yan W, Wu MH, Lin YN, Agno JE, Sharma M, Braun RE, Rajkovic A, Matzuk MM. TEX14 is essential for intercellular bridges and fertility in male mice. Proc Natl Acad Sci U S A. 2006; 103:4982–4987. [PubMed: 16549803]

Hemmerich P, Weidtkamp-Peters S, Hoischen C, Schmiedeberg L, Erliandri I, Diekmann S. Dynamics of inner kinetochore assembly and maintenance in living cells. J Cell Biol. 2008; 180:1101–1114. [PubMed: 18347072]

Hewitt L, Tighe A, Santaguida S, White AM, Jones CD, Musacchio A, Green S, Taylor SS. Sustained Mps1 activity is required in mitosis to recruit O-Mad2 to the Mad1-C-Mad2 core complex. J Cell Biol. 2010; 190:25–34. [PubMed: 20624899]

Huang H, Yen TJ. BubR1 is an effector of multiple mitotic kinases that specifies kinetochore: microtubule attachments and checkpoint. Cell Cycle. 2009; 8:1164–1167. [PubMed: 19282664]

Iwamori T, Iwamori N, Ma L, Edson MA, Greenbaum MP, Matzuk MM. TEX14 interacts with CEP55 to block cell abscission. Mol Cell Biol. 2010; 30:2280–2292. [PubMed: 20176808]

Kang YH, Park JE, Yu LR, Soung NK, Yun SM, Bang JK, Seong YS, Yu H, Garfield S, Veenstra TD, et al. Self-regulated Plk1 recruitment to kinetochores by the Plk1-PBIP1 interaction is critical for proper chromosome segregation. Mol Cell. 2006; 24:409–422. [PubMed: 17081991]

Khodjakov A, Pines J. Centromere tension: a divisive issue. Nat Cell Biol. 2010; 12:919–923. [PubMed: 20885417]

Kulukian A, Han JS, Cleveland DW. Unattached kinetochores catalyze production of an anaphase inhibitor that requires a Mad2 template to prime Cdc20 for BubR1 binding. Dev Cell. 2009; 16:105–117. [PubMed: 19154722]

Liu D, Vader G, Vromans MJ, Lampson MA, Lens SM. Sensing chromosome bi-orientation by spatial separation of aurora B kinase from kinetochore substrates. Science. 2009; 323:1350–1353. [PubMed: 19150808]

Liu ST, Rattner JB, Jablonski SA, Yen TJ. Mapping the assembly pathways that specify formation of the trilaminar kinetochore plates in human cells. J Cell Biol. 2006; 175:41–53. [PubMed: 17030981]

Malureanu L, Jeganathan KB, Jin F, Baker DJ, van Ree JH, Gullon O, Chen Z, Henley JR, van Deursen JM. Cdc20 hypomorphic mice fail to counteract de novo synthesis of cyclin B1 in mitosis. J Cell Biol. 2010; 191:313–329. [PubMed: 20956380]

Maresca TJ, Salmon ED. Intrakinetochore stretch is associated with changes in kinetochore phosphorylation and spindle assembly checkpoint activity. J Cell Biol. 2009; 184:373–381. [PubMed: 19193623]

Musacchio A, Hardwick KG. The spindle checkpoint: structural insights into dynamic signalling. Nat Rev Mol Cell Biol. 2002; 3:731–741. [PubMed: 12360190]

Musacchio A, Salmon ED. The spindle-assembly checkpoint in space and time. Nat Rev Mol Cell Biol. 2007; 8:379–393. [PubMed: 17426725]

Neef R, Gruneberg U, Kopajtich R, Li X, Nigg EA, Sillje H, Barr FA. Choice of Plk1 docking partners during mitosis and cytokinesis is controlled by the activation state of Cdk1. Nat Cell Biol. 2007; 9:436–444. [PubMed: 17351640]

Petrovic A, Pasqualato S, Dube P, Krenn V, Santaguida S, Cittaro D, Monzani S, Massimiliano L, Keller J, Tarricone A, et al. The MIS12 complex is a protein interaction hub for outer kinetochore assembly. J Cell Biol. 2010; 190:835–852. [PubMed: 20819937]

Przewloka MR, Zhang W, Costa P, Archambault V, D'Avino PP, Lilley KS, Laue ED, McAinsh AD, Glover DM. Molecular analysis of core kinetochore composition and assembly in Drosophila melanogaster. PLoS One. 2007; 30:e478. [PubMed: 17534428]

Qi W, Tang Z, Yu H. Phosphorylation- and polo-box-dependent binding of Plk1 to Bub1 is required for the kinetochore localization of Plk1. Mol Biol Cell. 2006; 17:3705–3716. [PubMed: 16760428]

Santaguida S, Tighe A, D'Alise AM, Taylor SS, Musacchio A. Dissecting the role of MPS1 in chromosome biorientation and the spindle checkpoint through the small molecule inhibitor reversine. J Cell Biol. 2010; 190:73–87. [PubMed: 20624901]

Santamaria A, Wang B, Elowe S, Malik R, Zhang F, Bauer M, Schmidt A, Sillje HH, Korner R, Nigg EA. The Plk1-dependent phosphoproteome of the early mitotic spindle. Mol Cell Proteomics. 2011; 10:M110 004457. [PubMed: 20860994]

Seong YS, Kamijo K, Lee JS, Fernandez E, Kuriyama R, Miki T, Lee KS. A spindle checkpoint arrest and a cytokinesis failure by the dominant-negative polo-box domain of Plk1 in U-2 OS cells. J Biol Chem. 2002; 277:32282–32293. [PubMed: 12034729]

Shah JV, Botvinick E, Bonday Z, Furnari F, Berns M, Cleveland DW. Dynamics of centromere and kinetochore proteins; implications for checkpoint signaling and silencing. Curr Biol. 2004; 14:942–952. [PubMed: 15182667]

Sinclair CS, Rowley M, Naderi A, Couch FJ. The 17q23 amplicon and breast cancer. Breast Cancer Res Treat. 2003; 78:313–322. [PubMed: 12755490]

Wan X, O'Quinn RP, Pierce HL, Joglekar AP, Gall WE, DeLuca JG, Carroll CW, Liu ST, Yen TJ, McEwen BF, et al. Protein architecture of the human kinetochore microtubule attachment site. Cell. 2009; 137:672–684. [PubMed: 19450515]

Wong OK, Fang G. Cdk1 phosphorylation of BubR1 controls spindle checkpoint arrest and Plk1-mediated formation of the 3F3/2 epitope. J Cell Biol. 2007; 179:611–617. [PubMed: 17998400]

Wong OK, Fang G. Plx1 is the 3F3/2 kinase responsible for targeting spindle checkpoint proteins to kinetochores. J Cell Biol. 2005; 170:709–719. [PubMed: 16129782]

HIGHLIGHTS

- Tex14 is recruited to kinetochores by Plk1
- Outer kinetochore markers fail to localize to kinetochores in the absence of Tex14
- Tex14 is required for kinetochore-microtubule attachment and accurate chromosome congression
- Plk1-dependent degradation of Tex14 regulates the metaphase to anaphase transition

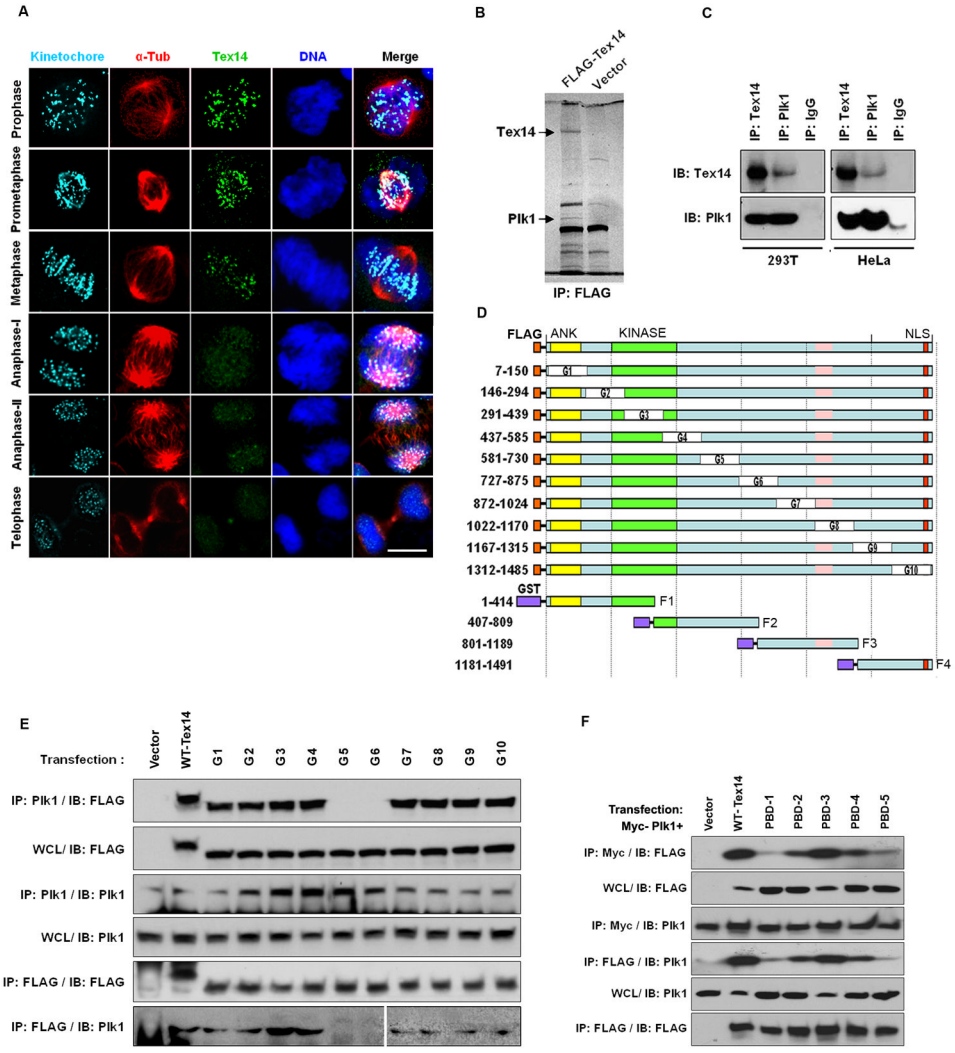

Figure 1. Cellular localization and interaction of Tex14 with Plk1

(A) Immunofluorescence staining of HeLa cells with Tex14 antibody during different phases of mitosis. Scale bar, 10μm. (B) Silver staining of Tex14 immunoprecipitates resolved in SDS-PAGE. (C) Co-immunoprecipitation (IP) and immunoblot (IB) analysis of nocodazole-treated 293T cells showing interaction between endogenous Tex14 and Plk1 proteins; IgG was used as non-specific control. (D) Schematic representations of predicted functional domains, deletion mutants (G1-G10 white boxes) and fragments of the Tex14 protein. Numbers refer to deleted amino acid residues. (E) Influence of Tex14 in-frame deletions (G1-G10, FLAG-tagged) on Tex14 interaction with endogenous Plk1 shown by co-IP and IB analysis of monastrol treated 293T cells as indicated; whole cell lysate (WCL). (F) Influence of Tex14 PBD mutations (FLAG-tagged) on the Tex14 interaction with Plk1. Co-IP and IB analysis of monastrol treated 293T cells expressing Tex14 proteins as indicated.

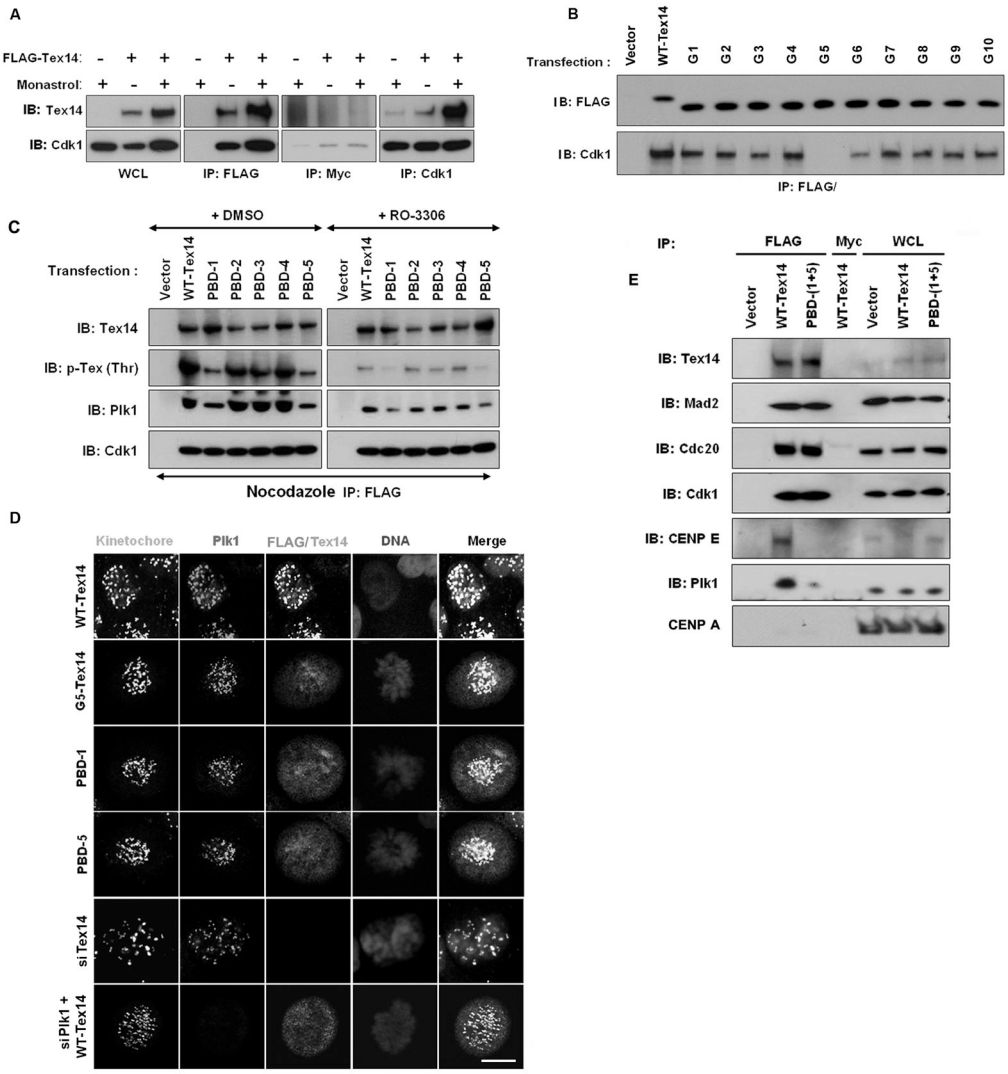

Figure 2. Cdk1-dependent interaction between Tex14 and Plk1

(A) Interaction of FLAG-tagged Tex14 with endogenous Cdk1 shown by co-IP and IB of monastrol-aligned 293T cells. (B) Cdk1 interacting sites on Tex14 identified by co-IPs and IB of monastrol treated 293T cells expressing FLAG-tagged Tex14 G1-G10 mutant proteins. (C) Influence of Tex14 PBD mutations and the Cdk1 inhibitor RO-3306 (5μM for 8hrs) on Plk1 and Cdk1 interactions with FLAG-tagged Tex14 proteins in Nocodazole treated 293T cells. (D) Immunolocalization of Plk1 and FLAG-tagged Tex14 wildtype and mutant proteins to KTs in 293T cells. siPlk1 and siTex14 served as negative controls. Scale bar, 10μm. (E) Interaction between FLAG-tagged wildtype and the PBD-(1+5) mutant of Tex14 and endogenous outer KT proteins in monastrol aligned 293T cells as indicated. Myc IP was used as a negative control.

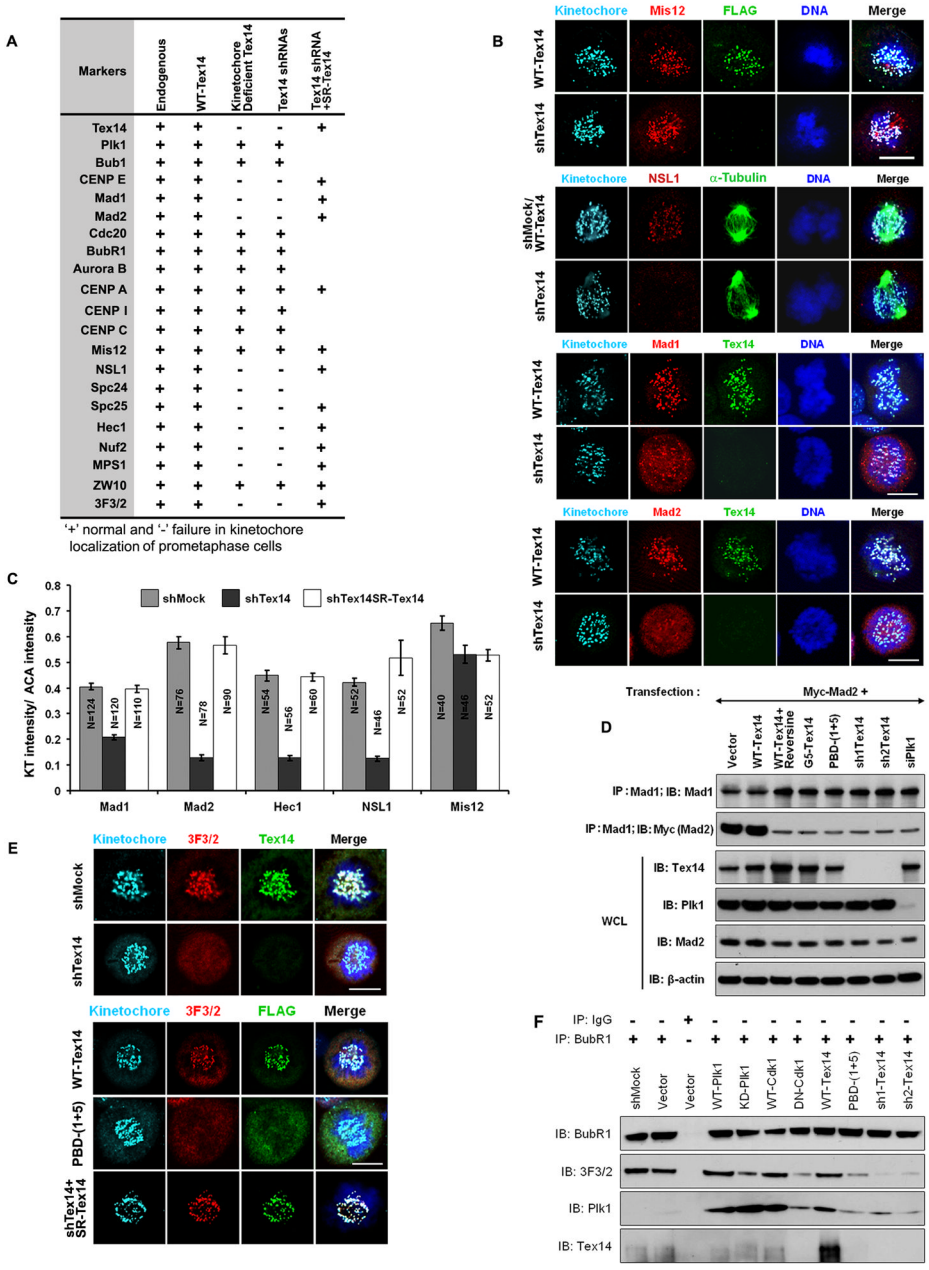

Figure 3. The influence of Tex14 on localization of KT markers

(A) Table summarizing KT localization of the indicated markers in HeLa cells in response to Tex14 modification; + and − refer to ability of the marker to localize to KTs. Kinetochore deficient Tex14 represents PBD-1, PBD-5 and PBD-(1+5) (B) Immunolocalization of indicated markers to KTs in response to shRNA depletion of Tex14. Kinetochores were detected by anti-centromere antibody (ACA). Tex14 staining was conducted with a FLAG-tage or Tex14 antibody. (C) Quantitation of mean kinetochore levels (intensity) for the indicated markers in response to Tex14 depletion (shRNA) and reconstitution with shRNA resistant Tex14 (SR-Tex14). Marker intensity was normalized to ACA levels. Error bars represent standard error of the mean (SEM). (D) Influence of Tex14 mutants, shRNAs and reversine on the Mad1-Mad2 interaction in nocodazole treated 293T cells. IP and IB antibodies are indicated. (E) KT immunolocalization of the 3F3/2 phospho-epitope in

response to Tex14 manipulation. Markers are shown. (F) The influence of Plk1, Cdk1 and Tex14 depletion or mutation on levels of endogenous BubR1-associated 3F3/2 phosphoepitope in monastrol treated 293T cells. Scale bars (B and E), 10μm.

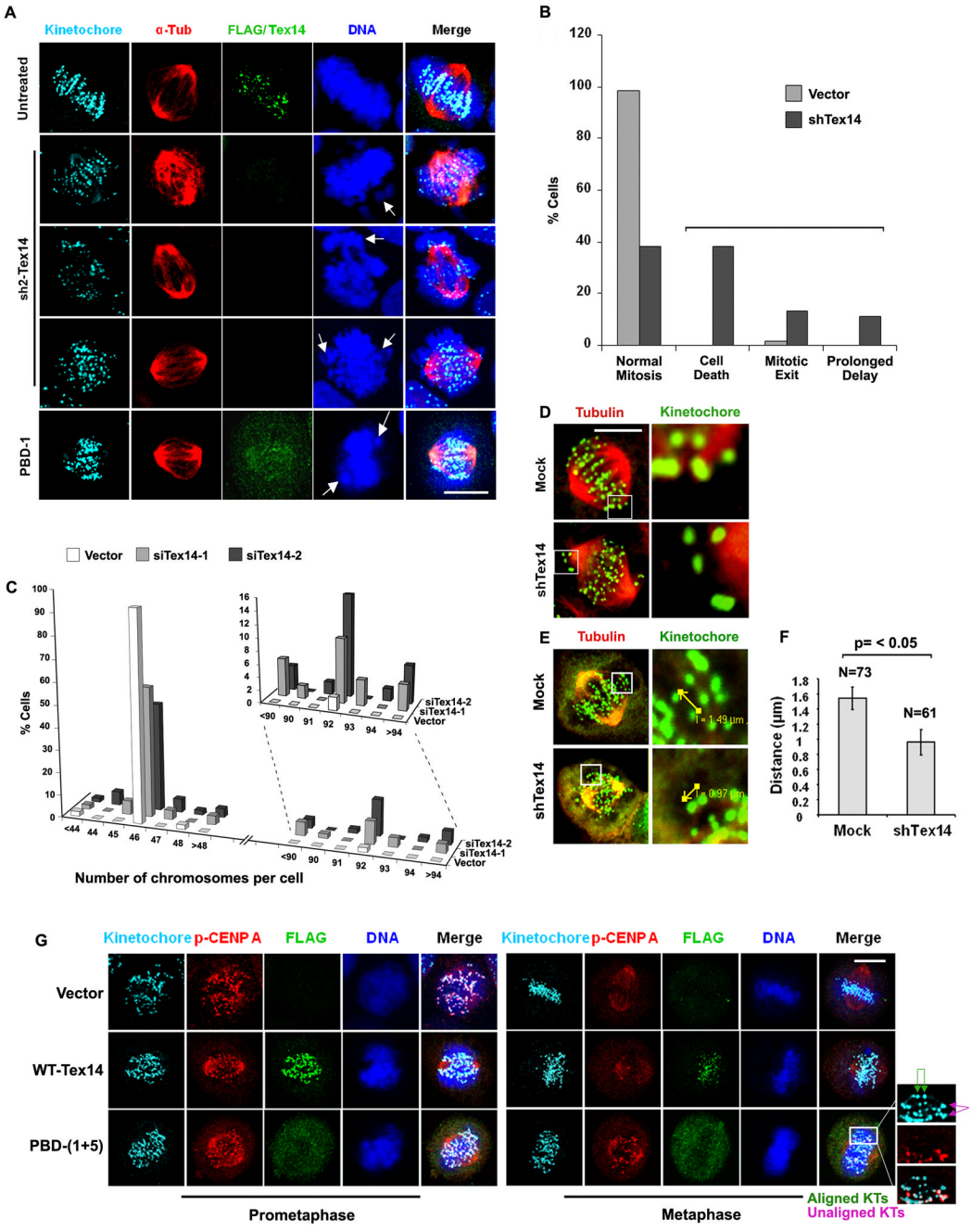

Figure 4. Mitotic defects associated with Tex14 depletion

(A) Chromosome congression defects in 293T cells following depletion or mutation of Tex14 shown by immunofluorescence. Chromosomal segregation defects are indicated by arrows. (B) Mitotic defects associated with Tex14 depletion detected by live cell imaging of 40-60 cells. (C) Aneuploidy and polyploidy in Tex14 depleted HCT116 cells defined by chromosome counts from 50 metaphase spreads. (D) High magnification images of KT-MT junctions in Tex14 depleted cells. (E) Inter-centromeric distance of paired KTs at metaphase in Tex14 depleted cells. (F) Average distance between paired KTs in Tex14 depleted cells. (G) Immunofluorescence for phospho-CENP-A during prometaphase and metaphase in cells

deficient in KT localization of Tex14; Magnified sections show retention of p-CENP-A on unaligned KTs. Scale bars (A and G), 10μm.

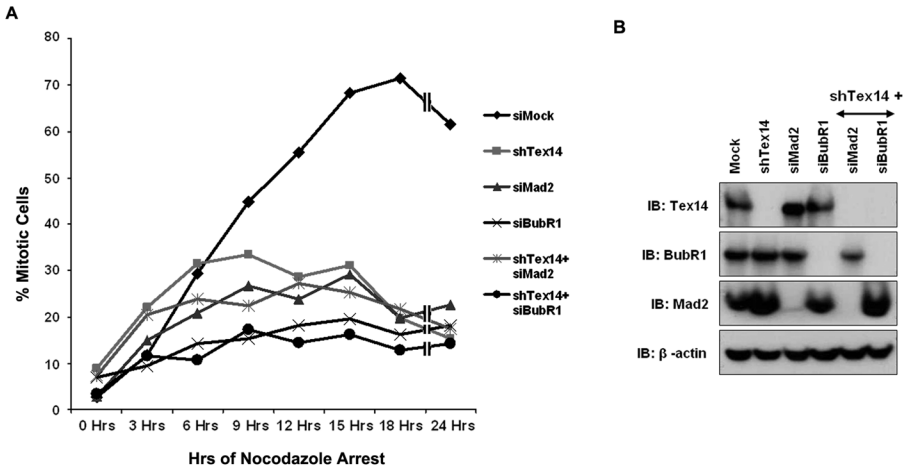

Figure 5. Influence of Tex14 depletion on SAC activity

(A) Quantitation of percent of cells (n=200) in mitosis in nocodazole treated HeLa cells following depletion of Tex14, Mad2 and BubR1 by siRNAs or shRNAs. (B) Immunoblot (IB) analysis of HeLa cells treated with Tex14, BubR1 and Mad2 specific siRNAs and shRNAs to verify reduced levels of associated proteins.

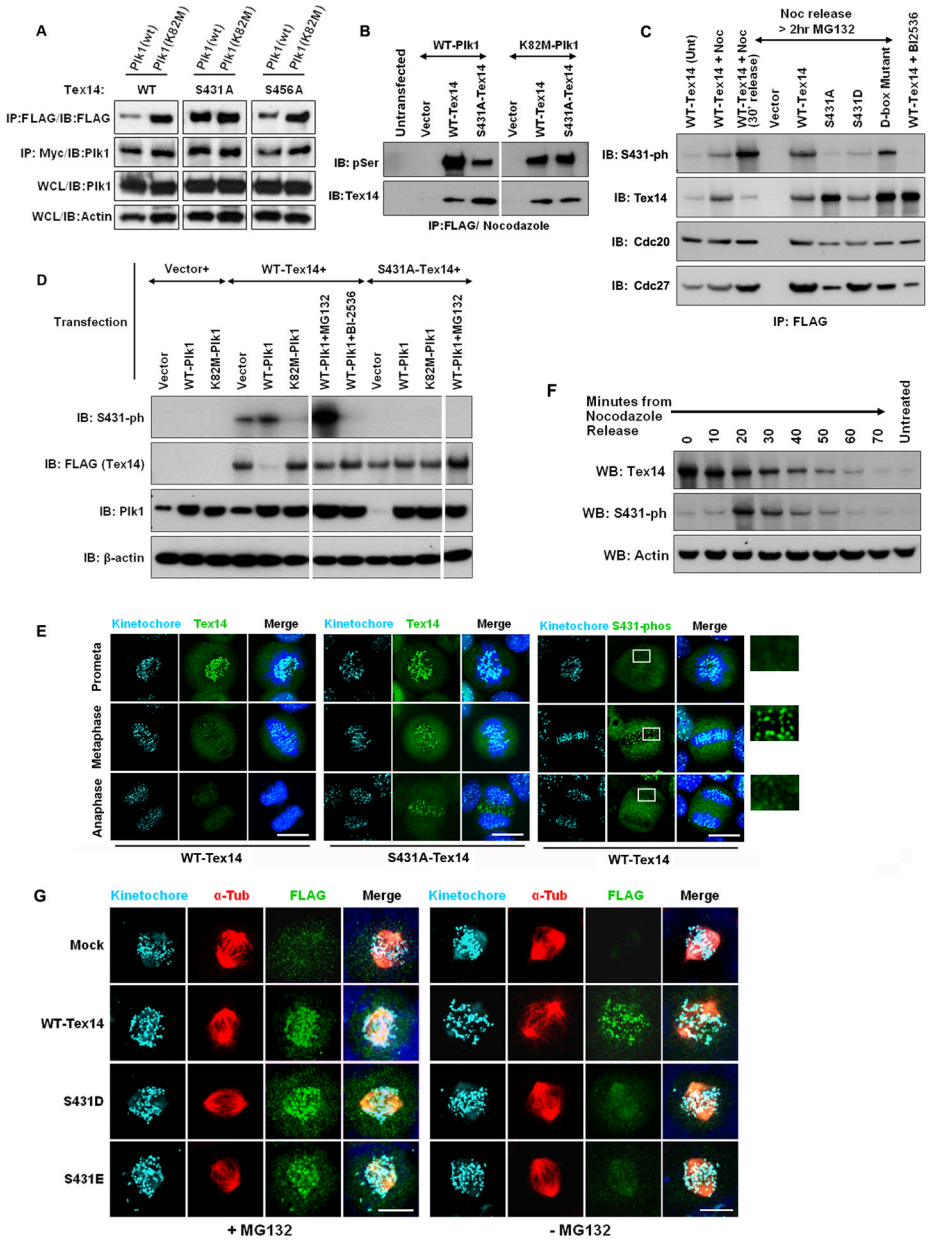

Figure 6. Phosphorylation of Tex14 by Plk1

A) Stabilization of Tex14 levels by DN-Plk1 and S431A-Tex14 shown by co-IP and IB analysis of nocodazole arrested 293T cells as indicated. Tex14 is FLAG-tagged, Plk1 is Myc-tagged. (B) Reduced serine phosphorylation of Tex14 and increased Tex14 levels in response to S431A mutation or DN-Plk1 as shown by co-IP and IB analysis of nocodazole arrested 293T cells as shown. Tex14 is FLAG-tagged. (C) Increased Tex14 S431 phosphorylation in 293T cells aligned in late prometaphase and metaphase by MG132 or Nocodazole shown by co-IP and IB analysis with S431 phospho-specific antibody. Tex14 S431A, S431D, and D-box mutants and the BI2536 Plk1 inhibitor result in increased Tex14 levels due to reduced S431 phosphorylation. Cdc20 and Cdc27 were used as mitotic controls. All Tex14 proteins are FLAG-tagged. (D) Dependence of the S431 phospho-

specific antibody on S431 of Tex14 and Plk1 activity shown by IB of 293T cells expressing wildtype or S431A-Tex14 and aligned by MG132. BI2536 Plk1 inhibitor served as a negative control for Plk1 phosphorylation. All Tex14 proteins are FLAG-tagged. (E) Immunolocalization of wildtype Tex14 and S431 phosphorylated Tex14 to KTs during mitosis using Tex14 and S431-phosphospecific antibodies. Magnified sections show S431-phosphorylation on metaphase KTs. (F) IB analysis of Tex14 and S431 phosphorylated Tex14 in 293T cells following release from nocodazole arrest. (G) Immunolocalization of wildtype and S431-phosphomimic mutant Tex14 in 293T cells during prometaphase and metaphase in response to the proteasome inhibitor MG132. All Tex14 proteins are FLAG-tagged. Scale bars (E and G), 10μm.

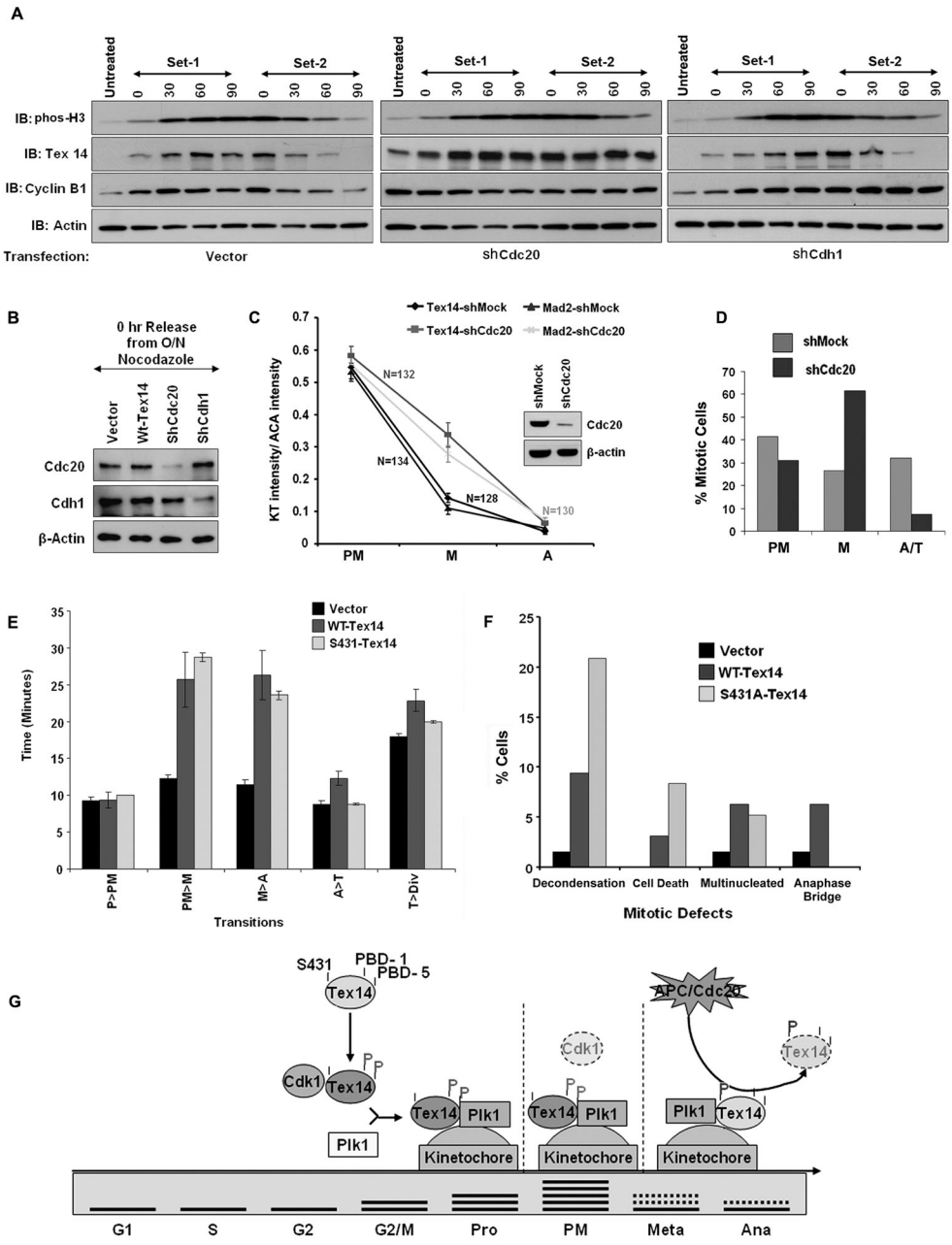

Figure 7. APC/C^{Cdc20} dependent degradation of Tex14

(A) Depletion of Cdc20 stabilizes Tex14 levels. Cdc20 and Cdh1 depleted 293T cells were synchronized by double thymidine and release into nocodazole (Set-1) or by nocodazole alone (Set-2) (see text for details). IB analysis shows levels of Tex14 and the phospho-Histone3 (H3) and Cyclin B1 mitotic markers at various times (min) in nocodazole (Set-1) or after nocodazole release (Set-2). (B) IB analysis showing depletion of Cdc20 or Cdh1 by shRNAs in nocodazole aligned 293T cells (Set-1). (C) Mean KT-intensity of Mad2 and Tex14, normalized by ACA intensity, in shCdc20 shRNA treated HeLa cells during prometaphase (PM), metaphase (M) and anaphase (A). Error bars represent the SEM. IB confirms reduced Cdc20 levels in response to shCdc20. (D) Percent cells with Tex14

staining at KTs from (C) in prometaphase (PM), metaphase (M) and anaphase (A) cells. (E) Average time between stages of mitosis detected by live cell time-lapse microscopy of 293T cells; 40-60 cells were analyzed for each condition. (F) Percentage of mitotic defects in H2B-mRFP-tagged 293T cells expressing wildtype or S431A-Tex14 detected by live cell time-lapse microscopy; 40-60 mitotic cells were scored for each condition. (G) Model illustrating biphasic regulation of Tex14 by Plk1 during mitosis. Number of horizontal lines in each phase of mitosis represents relative levels of Tex14.